Journal of Drug Targeting

ISSN: 1061-186X (Print) 1029-2330 (Online) Journal homepage: https://www.tandfonline.com/loi/idrt20

# Free radical-mediated targeting and immobilization of coupled payloads

Christopher J. Lowe, Emily T. DiMartini, Keana R. Mirmajlesi, Adam J. Gormley & David I. Shreiber

**To cite this article:** Christopher J. Lowe, Emily T. DiMartini, Keana R. Mirmajlesi, Adam J. Gormley & David I. Shreiber (2019): Free radical-mediated targeting and immobilization of coupled payloads, Journal of Drug Targeting, DOI: 10.1080/1061186X.2019.1584807

**To link to this article:** https://doi.org/10.1080/1061186X.2019.1584807

Accepted author version posted online: 20 Feb 2019.
Published online: 11 Mar 2019.

JOURNAL OF DRUG TARGETING
https://doi.org/10.1080/1061186X.2019.1584807

Taylor & Francis
Taylor & Francis Group

ORIGINAL ARTICLE



# Free radical-mediated targeting and immobilization of coupled payloads

Christopher J. Lowe, Emily T. DiMartini, Keana R. Mirmajlesi, Adam J. Gormley and David I. Shreiber

Department of Biomedical Engineering, Rutgers, The State University of New Jersey, Piscataway, NJ, USA

**ABSTRACT**

Targeted drug delivery is a promising approach to enhance the accumulation of therapies in diseased tissues while limiting off-site effects. Ligand-receptor interactions are traditionally identified to deliver therapies, and although specific, this can be costly and often suffers from limited sensitivity. An emerging approach is to target intermediary species that modulate disease progression. Here, we propose novel methods of targeting therapies by using native free radicals as a homing signal. Elevated concentrations of free radicals are a characteristic comorbidity of many different diseases. In polymer chemistry, free radicals are frequently used to initiate crosslinking reactions. We proposed that free radicals elevated in injury sites are capable of inducing crosslinking of acrylate groups on polymer chains. Coupling payloads to the polymer then allow for specific targeting of therapies to areas with elevated free radicals. We demonstrate *in vitro* proof-of-principle of this approach. Reactive oxygen species (ROS) initiated crosslinking of acrylated PEGs, which immobilized a fluorescent payload within tissue mimics. The cross-linking efficiency and immobilization potential varied with the polymer chain length, suggesting that a tuneable platform can be achieved. Together these results provide promising proof-of-concept for using free radicals to specifically target and sustain nearly endless payloads to disease sites.

**ARTICLE HISTORY**
Received 31 October 2018
Revised 29 January 2019
Accepted 14 February 2019

**KEYWORDS**
Free radicals; drug delivery; biomaterials; polymerisation; PEGDA

## Introduction

Targeted drug delivery offers the promise for the selective and precise delivery of drug payloads directly to the cells and tissues that require the therapeutic, which can minimise required dosages and off-target side effects [1]. Successful targeted drug delivery requires a balance of specificity and sensitivity. Various types of drug-carrying nanoparticles have been developed to carry a therapeutic agent to the target tissue following systemic delivery [2]. Most often, target-specific ligands are coupled to the nanoparticle surface to selectively bind to a single cell surface receptor [3–5]. In cancer treatment, receptors overexpressed on the tumour cell's surface are identified as substrates for ligand-receptor interactions [2–4,6]. However, because of the heterogeneity of different types of cancers, this approach requires the discovery of ligands that are unique to cell surface receptors on different types of tumours [1,2,4,6,7]. As such, new targets and ligands must be identified for any new application, which is both non-trivial and costly [5]. Further, tumours do not evenly express surface cell receptors throughout the tumour mass, and the expressed receptors continuously change [2,6]. The heterogeneity within tumours and between tumour types limits the therapeutic capabilities of a ligand-based targeting approach. Additionally, receptors that are overexpressed in tumour cells are also expressed to a lesser degree in healthy cells, which can lead to off-target dumping [1,6]. An approach that does not target cells but rather a species that is produced under pathologic situations may allow for targeted delivery to be applied to a broader range of injury and disease conditions.

Candidates for targeting a broader array of disorders are free radicals. Elevated concentrations of free radicals are characteristic of a wide variety of tissue injuries and disease states, including inflammatory diseases, neurological disorders, ischaemic diseases, burn wounds, cancer, organ transplantation, and traumatic brain injuries [8–14]. Free radicals are species left with at least one unpaired electron, which renders them extremely reactive and capable of causing significant damage to proteins, lipid membranes, nucleic acids, and other critical cellular components [12]. Free radicals that are produced natively in the body include hydroxyl ($OH^{\bullet}$), superoxide ($O_2^{\bullet -}$), nitric oxide ($NO^{\bullet}$), and lipid peroxyl (lipid-$OO^{\bullet}$) [9]. Although not free radicals themselves, hydrogen peroxide ($H_2O_2$), peroxynitrate ($ONOO^-$), and other species are categorised as oxidants that can mediate free radical reactions or be decomposed into free radicals themselves [10,12]. Low levels of free radicals are continuously present *in vivo* and play a crucial role in many cellular functions, such as combating infectious organisms and serving as messengers in cell signalling cascades [12,15,16]. A delicate steady state exists between formation of free radicals *in vivo* and their detoxification through natural antioxidant mechanisms. In injured and diseased tissues, the production of free radicals is often greatly increased, thereby overwhelming native antioxidant mechanisms and resulting in persistently elevated concentrations of free radicals in afflicted tissues and associated damage [12].

Although the heightened reactivity of free radicals can be deleterious *in vivo*, it serves as a valuable tool in polymer chemistry to initiate and control crosslinking or polymerisation of a variety of chemical functional groups [17]. For example, acrylate groups are one type of functional group that is increasingly used in biomedical applications that can be crosslinked in the presence of free radicals [18]. We hypothesised that the elevated production of free radicals in injured and diseased tissues is capable of inducing crosslinking of acrylate groups. If sufficient crosslinking occurs, the polymers will become too large to diffuse out of the tissue, thereby targeting their accumulation as well as any therapeutic

**CONTACT** David I. Shreiber shreiber@soe.rutgers.edu Department of Biomedical Engineering, Rutgers, The State University of New Jersey, 599 Taylor Road, Piscataway, NJ, USA

factors that are coupled to the original acrylated molecules to the areas of high free radical production. By providing a substrate for the free radicals, these polymers may also provide a measure of free radical scavenging to further protect tissues as an anti-oxidant.

Reaction conditions can be controlled during benchtop chemical synthesis to maximise crosslinking and polymerisation efficiency. In contrast, to achieve our goal of initiating crosslinking and immobilization *in vivo*, we must adapt the materials and understand their reactions in a physiological environment with much less control. To that end, a robust characterisation of different starting materials and how they react with free radical species commonly encountered *in vivo*, particularly reactive oxygen species (ROS) and reactive nitrogen species (RNS), is necessary [19–20]. In this paper, we evaluate the potential to use ROS and RNS to initiate crosslinking and promote immobilization of acrylated polymers.

## Materials and methods

### Materials

Two thousand Dalton PEG (84797), 2000 Dalton PEG monoacrylate (730270), and 1000 Dalton (729086), 2000 Dalton (701971), 6000 Dalton (701963), and 10,000 Dalton (729094) PEG diacrylate were purchased from Sigma Aldrich. 2,2-Diphenyl-1-picrylhydrazyl (D9132), horseradish peroxidase (P8375), S-Nitroso-N-acetyl-DL-penicillamine (N3398), hydrogen peroxide (216763), acetylacetone (P7754), deuterated chloroform (151823), Hepes buffer (H3537), L-glutamine (G7513), Penicillin-Streptomycin (P4458), and DMEM (D5546) were also purchased from Sigma Aldrich. Griess Reagent Kit (G7921), Neurobasal Media (21103–049), and B-27 Supplement (17504044) were purchased from ThermoFisher. 2k Acrylate-PEG Rhodamine and 2k Acrylate-PEG-FITC were synthesised by Creative PEGworks on a custom basis. Type-I bovine collagen (C857) was purchased from Elastin Products Company. Irgacure 2959 was the generous gift of the BASF Corporation.

### DPPH assay

Samples of acrylated PEG across a range of molecular weights were dissolved in water at the target concentrations before adding 50 μM 2,2-Diphenyl-1-picrylhydrazyl (DPPH) in methanol. Thirty minutes after addition of the DPPH to acrylated PEG samples, absorbance at 517 nm was measured using a Tecan Infinite M200 Pro.

### ROS assay

Generation of ROS was accomplished by combining hydrogen peroxide ($H_2O_2$) with horseradish peroxidase (HRP). A 50:50 mixture of $H_2O_2$ and tetramethylbenzidine (TMB) solution (BD OptEIA TMB Substrate Kit – Fisher Scientific) was combined with the sample condition being evaluated. A solution of HRP at 0.1 μg/mL was added to initiate formation of ROS. The reaction was allowed to run for 60 s before a stop solution of 1 M sulphuric acid was added to halt further progression of the assay. Absorbance was read at 450 nm and 540 nm on a Tecan Infinite M200 Pro. Background signal at 540 nm was subtracted from signal at 450 nm, per the TMB substrate kit instructions.

### RNS (SNAP) assay

Interaction of acrylated PEG with RNS was evaluated with the use of S-Nitroso-N-acetyl-DL-penicillamine (SNAP). SNAP was dissolved in phenol red-free Neurobasal media (Life Technologies) and combined with samples of acrylated PEG at target concentrations and then incubated at 37 °C and 5% $CO_2$ for 24 h. Following incubation, nitrite concentration was evaluated via the Griess reaction. Samples were prepared by combining 172 μl DI water with 63 μl of the nitrite-containing sample. This solution was then combined with 20 μl of Griess reagent (ThermoFisher). Griess reagent was prepared by combining equal volumes of sulphanilic acid and N-(2-naphthyl)ethylenediamine dihydrochloride per manufacturer's instructions. Solution absorbance was read at 548 nm on a Tecan Infinite M200 Pro following 30-min incubation.

### Size exclusion chromatography (GPC) experiments

Samples of 20 mg/mL acrylated PEG of various molecular weights were reacted overnight in PBS with 0, 4, 8, or 12 mg/mL HRP in the presence of 80 μM $H_2O_2$ and 120 μM acetylacetone (ROS initiators) or 3 mM SNAP (RNS initiator). Following reaction, GPC samples were resuspended in 0.02% $NaN_3$ in 0.5× PBS at 2 mg/mL and run through the column at 0. 5 ml/min using an Agilent 1200 GPC with UV, RI and light scattering (miniDAWN TREOS II, Wyatt Technology) detectors. Molecular weight for PEG species was estimated using an EasiVial PEG/PEO, pre-weighed calibration kit (Agilent Technologies). Peak height was used to calculate percent conversion, which was reported as the average of three experiments.

### Nuclear magnetic resonance (NMR) spectroscopy measurements

Polymer samples for NMR were reacted overnight as described in GPC experiments. NMR samples were lyophilised and resuspended in deuterated chloroform. NMR spectra were obtained with a Bruker Avance III 600 MHz.

### Acryated PEG immobilization within collagen hydrogels

Type-I bovine collagen (Elastin Products Company) was reconstituted in 0.02 N acetic acid at 3 mg/mL. Buffered hydrogel solutions were prepared using the following protocol for 1 ml: 20 μL HEPES, 130 μL 0.15 N NaOH, 100 μL 10x PBS, 73 μL 1x PBS, and 677 μL collagen solution. For photoinitiator conditions, 0.1 wt% Irgacure 2959 (BASF), a UV-sensitive photoinitiator, was included in the buffered hydrogel solution. Hydrogel solutions were allowed to self-assemble at 37 °C for 2 h. Acrylated PEG samples doped with 1% v/v 2000 Da acrylate-PEG-rhodamine or acrylate-PEG-FITC (Creative PEG Works) were added to the hydrogels and allowed to diffuse throughout the gel overnight. Following hydrogel self-assembly and diffusion of PEG solutions, the hydrogels were exposed to UV light for 5 min to initiate formation of radicals from the photoinitiator. For ROS conditions, HRP was added to the buffered hydrogel solution. Following hydrogel self-assembly and diffusion of PEG solutions, $H_2O_2$ and acetylacetone were added to the gels to initiate ROS formation and allowed to react for 24 h. For both free radical types investigated, a series of five 3-h washes with PBS were performed after reaction with free radicals. The residual fluorescence of the hydrogels after all washes were measured (Rhodamine: excitation 540, emission 568; FITC: excitation 495, emission 525) using a Tecan Infinite M200 Pro Plate Reader.

### *Rat dermal fibroblast culture and cellular protection studies (cytotoxicity and protection)*

Rat dermal fibroblasts (RDFs) that constitutively expressed green fluorescent protein (GFP) were isolated from a transgenic animal (a gift from the W.M. Keck Center for Collaborative Neuroscience). RDFs were cultured in DMEM 5546 containing 10% FBS, 1% L-glutamine, and 1% penicillin/streptomycin and seeded onto 96-well plates at a density of 1500 cells/well. For cytotoxicity studies, acrylated PEG treatments were dissolved in fresh culture media, then added directly to RDF cultures and allowed to incubate for 24 h. Cellular metabolic activity was then evaluated using the Vybrant MTT assay (Life Technologies) according to the manufacturer's instructions. For cellular protection studies, acrylated PEG treatments were added simultaneously with 600 μM $H_2O_2$ and allowed to incubate for 24 h. Metabolic activity was again measured using the MTT assay.

### *Rat cortical neuron culture and cellular protection studies (cytotoxicity and protection)*

Rat cortical neurons were isolated from a timed pregnant animal at embryonic day 18 as described in the literature via techniques previously used in our laboratory under an approved IACUC protocol [21]. Neurons were cultured in Neurobasal media containing 2% B-27 supplement, 1% KCl, 1% penicillin/streptomycin, and 0.5% L-glutamine and seeded into 96 well plates at a density of 100,000 cells/well. For cytotoxicity studies, acrylated PEG treatments were dissolved in fresh culture media without B-27 added, then added directly to cortical cultures and allowed to incubate for 24 h. Cellular metabolic activity was then evaluated using the Vybrant MTT assay (Life Technologies) according to the manufacturer's instructions. For cellular protection studies, acrylated PEG treatments were added simultaneously with 20 μM $H_2O_2$ or 10 μM $H_2O_2$ and allowed to incubate for 24 h. Metabolic activity was again measured using the MTT assay.

## Results

### *Free radical reactivity*

The reactivity of PEGDA with the DPPH, ROS, and RNS free radicals is presented in Figure 1.

### *DPPH Assay*

DPPH is a stable radical with a characteristic purple colour and peak absorbance at 517 nm [22]. Upon reduction, DPPH loses its purple colour and commensurate absorbance at 517 nm. Changes in absorbance at this wavelength are shown in Figure 1(A) and can be used to monitor the oxidative state of DPPH. Ascorbic acid, a known antioxidant and free radical scavenger, reduced the concentration of DPPH radicals to less than 10% of initial levels, even at very low concentrations. Acrylated PEG across a variety of molecular weights also reduced the absorbance of the DPPH molecule. The highest concentrations of PEGDA examined reduced DPPH to 20–40% of initial levels. When non-acrylated PEG was reacted with DPPH, absorbance of the DPPH molecule remained unchanged, regardless of the concentration of PEG added.

### *ROS Assay*

Reactivity of acrylated PEG with ROS was assessed as a competition assay with TMB as the alternative substrate. Increasing

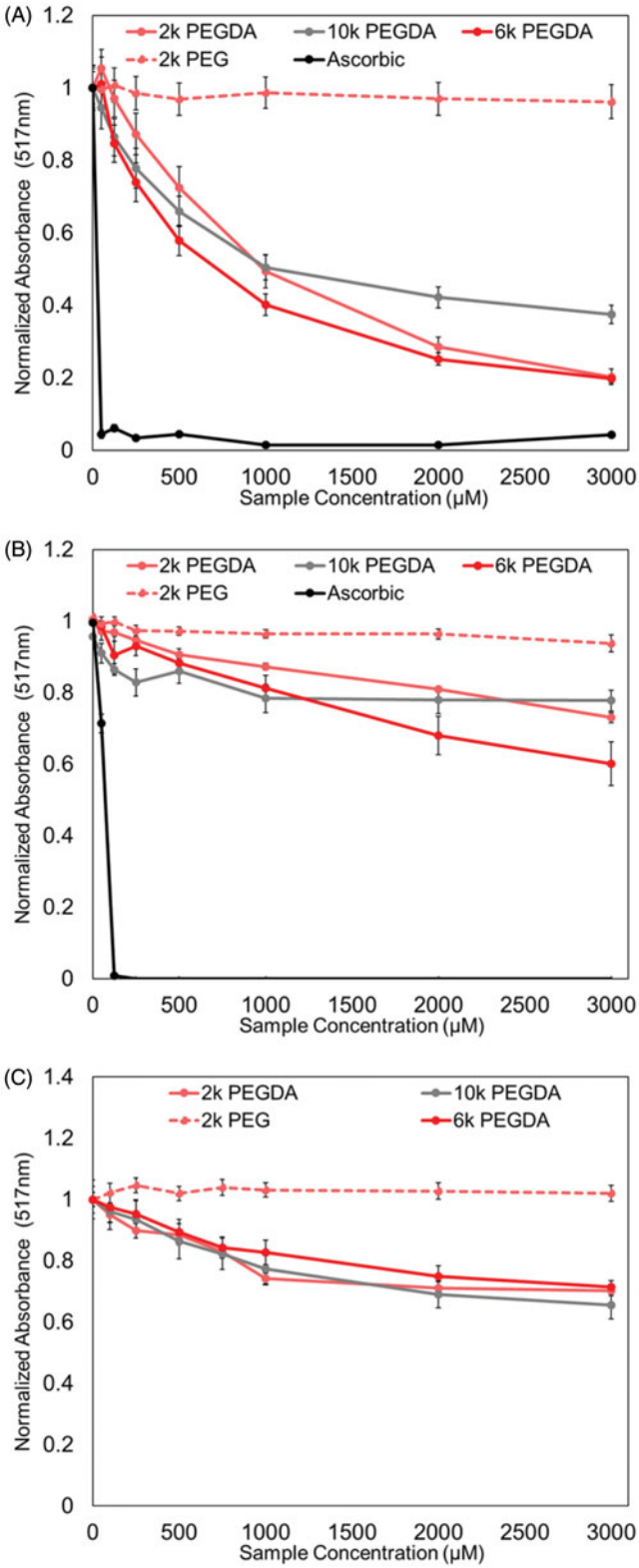


**Figure 1.** Free Radical Activity Assays for Acrylated PEGs (A) Absorbance Measurements from DPPH Assay Following Treatment with Acrylated PEGs. Increasing amounts of acrylated PEGs decrease the absorbance of DPPH, whereas nonacylated PEGs do not. Ascorbic acid is included as a positive control and substantially reduces DPPH absorbance even at low concentrations. (B) Absorbance Measurements from ROS Assay Following Treatment with Acrylated PEGs. Increasing amounts of acrylated PEGs decrease the absorbance of TMB, whereas nonacylated PEGs do not. Ascorbic acid is included as a positive control and substantially reduces TMB absorbance even at low concentrations. (C) Absorbance Measurements from RNS Assay Following Treatment with Acrylated PEGs. Increasing amounts of acrylated PEGs decrease the absorbance of the Griess reagent, whereas nonacylated PEGs do not. Ascorbic acid was not able to be included because it interferes with the Griess reaction.

concentrations of acrylated PEG resulted in decreased colour development and lower absorbance (Figure 1(B)). Ascorbic acid reduced the concentration of ROS radicals to negligible levels, even at very low concentrations. Acrylated PEG from 2000 to 10,000 Daltons reduced the TMB absorbance produced by the ROS radicals by 20–40%. When non-acrylated PEG was reacted with ROS, TMB absorbance was unaffected, regardless of the concentration of PEG.

### *RNS Assay*

Increasing concentrations of acrylated PEG resulted in decreased nitrite concentrations as observed via the Griess reaction. The highest concentrations of acrylated PEG examined resulted in approximately 30% reduction of nitrite concentration across all molecular weights examined (Figure 1(C)). The presence of non-acrylated PEG had no observable effect on the concentration of nitrites. Ascorbic acid has been documented to interfere with the Greiss Reaction, thus ascorbic acid controls were not able to be included in this study [23].

### *NMR spectroscopy*

Unreacted monoacrylated PEG displayed strong signal from acrylate groups, as observed by the triplet at ~6 ppm (Figure 2). After reaction with ROS, the signal from that acrylate triplet was substantially reduced, indicating those acrylate groups have been consumed. Conversely, after reaction with RNS, the signal from the acrylate triplet remained unchanged, indicating that those acrylate groups have persisted.

### *Size exclusion chromatography*

PEG (2,000 dalton - 2k PEG), monoacrylated PEG (2,000 dalton - 2k PEG1A), and diacrylated PEG (2000, 6000, and 10,000 Dalton - 2k PEGDA, 6k PEGDA, 10k PEGDA) were reacted with varying concentrations of HRP in the presence of $H_2O_2$ and acetylacetone (Figure 3). In the absence of ROS (0 mg/mL HRP), a single defined peak was observed, which corresponded to the starting molecular weight of the polymer (2k PEG $M_w$: 1885, PDI:1.047; 2k PEG1A $M_w$:1813, PDI:1.053; 2k PEGDA $M_w$:1779, PDI:1.052; 6k PEGDA $M_w$:5843, PDI:1.024; 10k PEGDA $M_w$:10667, PDI:1.019). In all PEG sample curves, a peak at ~27 min elution time emerged and grew in intensity with increasing HRP (Figure 3(A)). Analysis of this HRP peak via light scattering estimated the size of this species as ~53,000 daltons using a dn/dc value of 0.185. As HRP concentration increased, the intensity of the initial polymer peak decreased while the intensity of doublet peaks increased (Figure 3 (C–E)), which indicates that higher order molecules were begin generated from the acrylated molecules. Changes in peak height were utilised to calculate percent conversion of the polymer as displayed in Table 1.

### *Polymer immobilization*

To develop the collagen hydrogel immobilization model, radicals were first introduced using the photoinitiator Irgacure 2959, which was incorporated into the collagen gel during hydrogel formation. Acrylate-PEG-rhodamine was also included, and the residual fluorescence intensity was read after washing of the collagen gel. Without PEGDA, substantial decreases in fluorescence occurred following UV exposure for PBS and 2k PEG conditions, even prior to washing, presumably indicating destruction of the fluorophore by the free radicals (Figure 4). When PEGDA was included, the

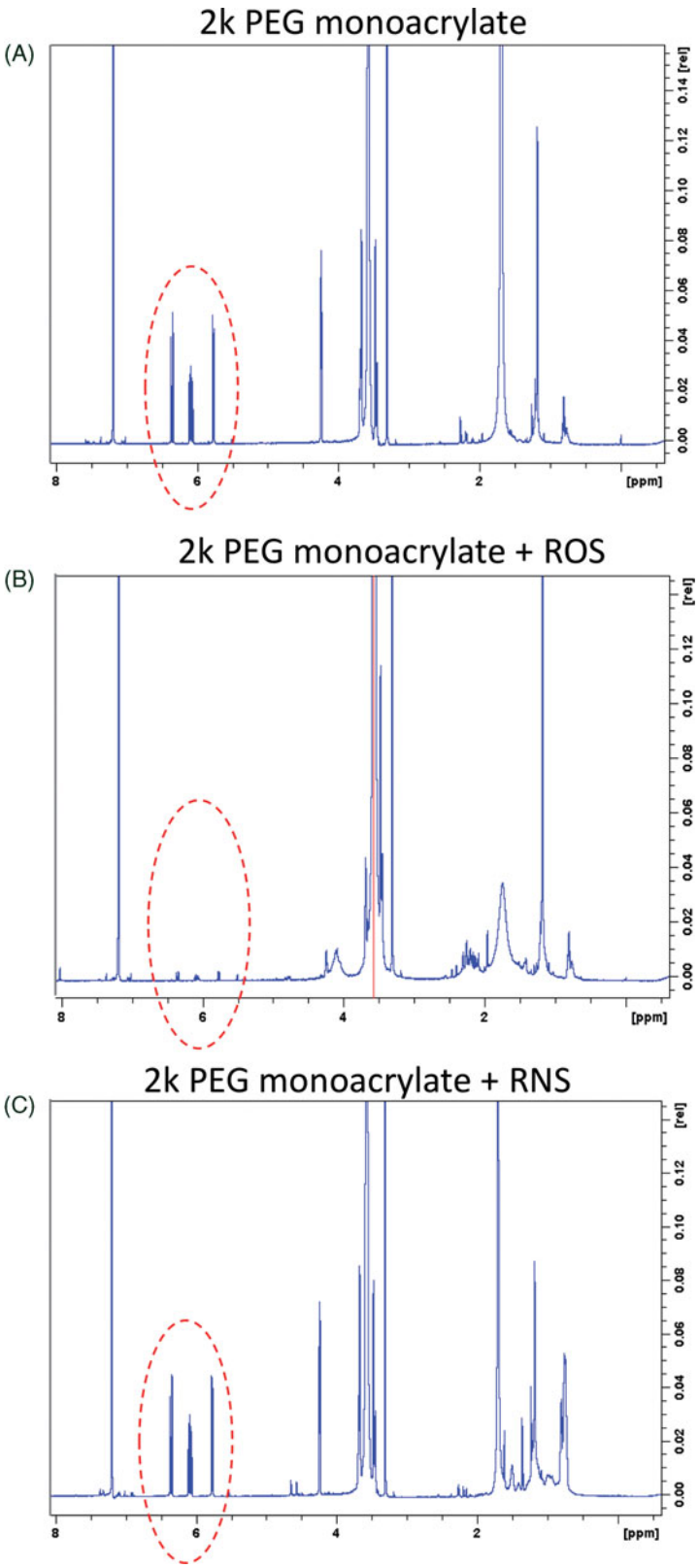


Figure 2. NMR Spectra of Acrylated PEGs Treated with ROS and RNS. NMR spectra for 2k PEG monoacrylate (left) shows strong signal from acrylate groups (red dashed circles). After reaction with ROS (middle), the signal from acrylates is greatly reduced. Conversely, after reaction with RNS (right), the acrylate signal persists unchanged.

decrease in fluorescence as a result of UV exposure was minimal. Following extensive washing, the residual fluorescence for PEGDA conditions was higher than the untreated, PBS condition. Further, there was an increasing trend between molecular weight of

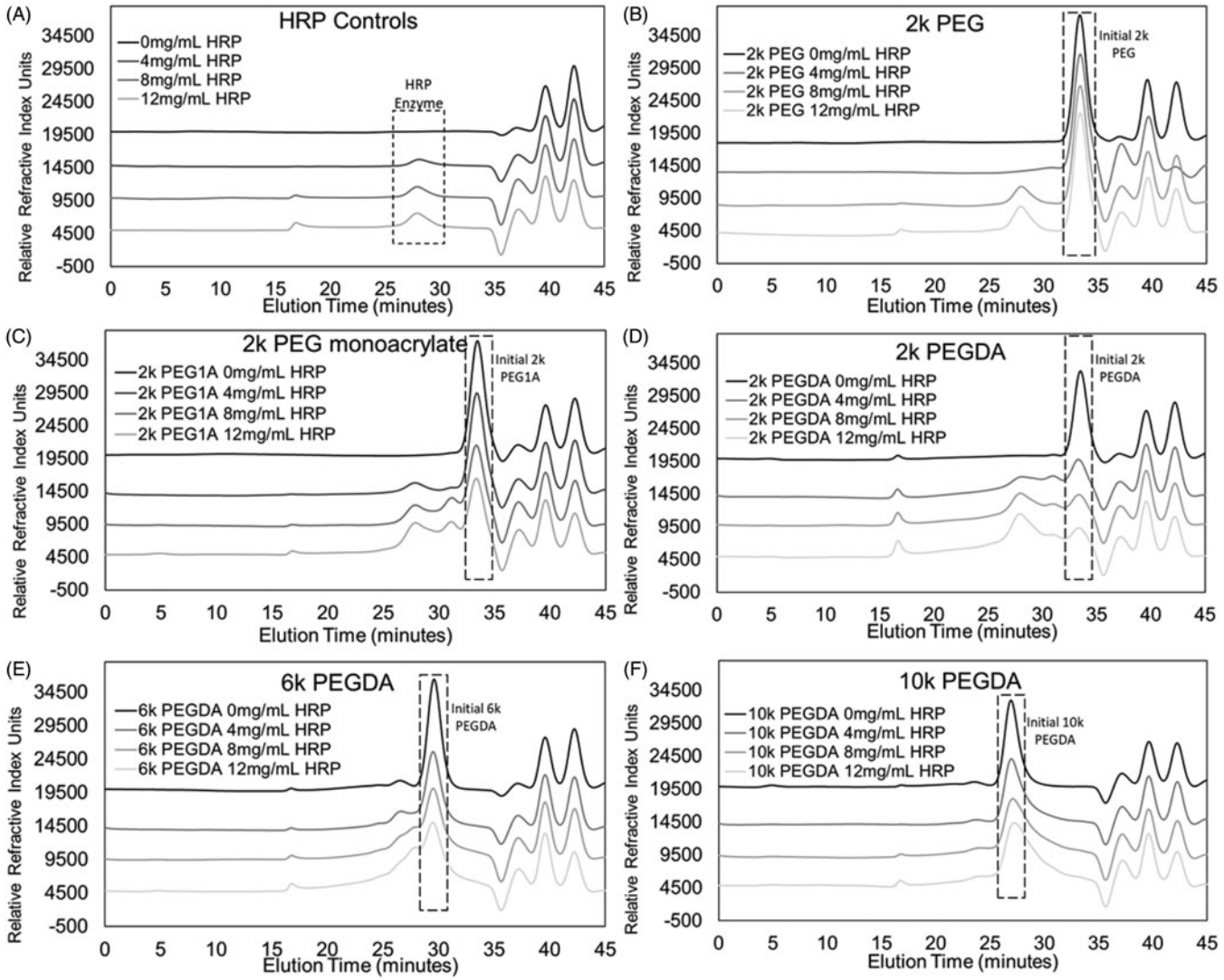


**Figure 3.** GPC Measurements for Acrylated PEGs Treated with ROS. GPC was used to characterise changing size distributions of acrylated PEGs when treated with increasing amounts of ROS. Increasing concentrations ROS were introduced by increasing the amount of HRP present for a given amount of $H_2O_2$ and acetylacetone. Control curves containing ROS components absent PEGs are presented in frame A. No change in size distribution was observed when non-acrylated PEGs were used (B). Increases in HRP concentration corresponded to a decrease in the intensity of the initial unreacted polymer peak and a simultaneous increase in the peak intensity of higher molecular weight species for 2k PEG monoacrylate (C), 2k PEGDA (D), 6k PEGDA (E), and 10k PEGDA (F).

**Table 1.** The percent conversion of polymer after reaction with ROS. Percent conversion was calculated by dividing peak height for each concentration of HRP by the peak height at 0 mg/mL HRP for each respective polymer and subtracting that from 1, with $N = 3$. [$\text{Conversion}_{\text{nHRP}} = 1 - (\text{PeakHeight}_{\text{nHRP}}/\text{PeakHeight}_{\text{0HRP}})$].

| HRP Conc. | 2k PEG | 2k PEG1A | 2k PEGDA | 6k PEGDA | 10k PEGDA |
|---|---|---|---|---|---|
| 0 mg/mL | 0% | 0% | 0% | 0% | 0% |
| 4 mg/mL | 2.31% (±4.72) | 13.2% (±3.32) | 61.3% (±2.63) | 22.7% (±7.49) | 26.0% (±1.55) |
| 8 mg/mL | 0.486% (±5.37) | 30.9% (±3.71) | 61.9% (±6.33) | 32.3% (±3.17) | 30.0% (±3.11) |
| 12 mg/mL | 4.27% (±1.83) | 32.4% (±5.67) | 62.3% (±4.69) | 31.6% (±4.88) | 29.7% (±3.07) |

the PEGDA and residual fluorescence – that is, the 10k PEGDA conditions displayed higher residual fluorescence than both the 6k and 2k PEGDA conditions. 6k PEGDA and 10k PEGDA conditions were significantly greater than the PBS (no UV) condition ($p < .0001$). 2k PEG and PBS conditions displayed low residual fluorescence, due in part to the substantial reduction in starting fluorescence observed after UV exposure but before washing.

To test the effects of ROS on PEGDA immobilization within the collagen hydrogels, HRP was incorporated into the hydrogel, and $H_2O_2$ + acetylacetone were added following diffusion of the polymers into the hydrogel. A slight decrease in fluorescence was observed when ROS were produced. Despite this, no conditions were significantly different than PBS without ROS prior to washing except for 2k PEG ($p = .0178$). Following all washes, the highest levels of residual fluorescence were observed in conditions with acrylated PEGs (Figure 4). Residual fluorescence for 10k PEGDA and 6k PEGDA conditions were significantly greater than PBS (no ROS), PBS, and 2k PEG conditions ($p < .0001$). Residual fluorescence for the 2k PEGDA condition was slightly greater than 2k PEG but less than that observed for 6k PEGDA and 10k PEGDA.

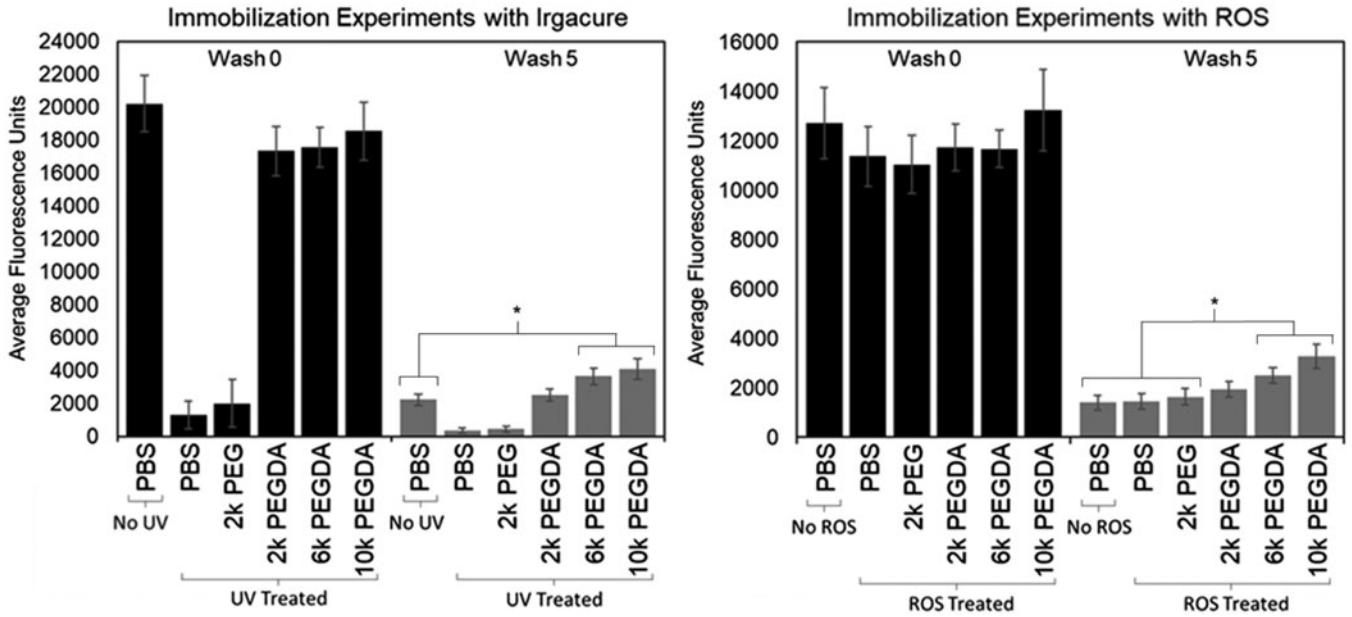


Figure 4. Immobilization of Acrylated PEGs within Collagen Hydrogels After Reaction with Free Radicals. Residual fluorescence of hydrogels was measured after reaction with Irgacure radicals (left) and ROS (right). Measurements were taken after reaction with radicals, but before any washes (Wash 0) and after all washes were completed (Wash 5). Exposure to radicals substantially reduced the fluorescence of rhodamine for Irgacure conditions, even before washes. 6k and 10k PEGDA showed significantly greater residual fluorescence as compared to PBS controls that were not exposed to radicals. For ROS studies, the presence of ROS did not substantially reduce the fluorescence of rhodamine before washes. 6k and 10k PEGDA showed significantly greater residual fluorescence as compared to 2k PEG, PBS, and PBS without radical exposure.

### *Cellular cytotoxicity and protection studies*

To assess the potential for these molecules to scavenge or otherwise protect cells from oxidative damage, cytotoxicity and cell protection studies were performed. First, the metabolic activity of RDFs and cortical neurons in the presence of acrylated PEGs and ascorbic acid controls were evaluated with the MTT assay without any free radical sources. For acrylated PEG conditions at or below 1000 μM, RDFs maintained greater than 88% of cellular metabolic activity as compared to untreated controls (Figure 5). Acrylated PEG concentrations of 1000 μM and above demonstrated more substantial drop-offs in metabolic activity. These trends were mirrored in ascorbic acid controls; at concentrations less than or equal to 1000 μM, metabolic activity was preserved. Cortical neurons were able to tolerate concentrations of acrylated PEG and ascorbic acid up to concentrations of 500 μM without decreases in cellular metabolic activity. At concentrations of 1000 μM and greater, cellular metabolic activity was decreased as compared to untreated controls (Figure 6).

In cellular protection assays with RDFs, introduction of 600 μM $H_2O_2$ induced a substantial decrease in cellular metabolic activity when acrylated PEG was not present. Adding increasing amounts of acrylated PEG or ascorbic acid protected RDFs from peroxide injury up to a concentration of 500 μM (Figure 5). Concentrations greater than 500 μM reduced cellular metabolic activity. For cellular protection studies with cortical neurons, addition of 20 μM and 10 μM $H_2O_2$ resulted in approximately 40% and 20% reductions in cellular metabolic activity respectively. Addition of acrylated PEG or ascorbic acid reduced the damaging effects of $H_2O_2$ up to concentrations of ~250 μM. Higher concentrations further reduced cellular metabolic activity (Figure 6).

## Discussion

Herein, we have demonstrated proof-of-concept *in vitro* for utilising native free radicals as a targeting signal to deliver and immobilize therapeutic factors at an injury site. Free radical generators that are commonly used to initiate polymerisation and crosslinking reactions in polymer chemistry and biomaterials science are typically not compatible with an *in situ* assembly approach due to their cytotoxicity. Although UV photoinitiators such as Irgacure are commonly used in biomedical application because they can be used under physiologic conditions, there are still substantial cytotoxic effects that must be considered [24]. We hypothesised that free radicals that exist naturally *in vivo* during injury and disease can serve to initiate crosslinking of acrylate groups *in situ*. We have presented preliminary evidence that (1) acrylated PEGs react with free radicals commonly observed *in vivo*, (2) the reaction of ROS with acrylated PEGs results in the covalent crosslinking of acrylate groups to one another, increasing their effective size, (3) acrylated PEGs can become trapped within a fibrillar collagen hydrogel tissue mimic following reaction with free radicals, and (4) acrylated PEGs can protect cells from oxidative stress *in vitro*. Collectively, these results represent a positive first step towards establishing a new targeted drug-delivery strategy amenable to a wide range of disease and injury states and therapeutic payloads.

The reactivity of acrylated PEG with three different radical species – DPPH, ROS, and RNS – was evaluated with colourimetric assays. The preliminary characterisation was performed with the DPPH assay, which is commonly used to evaluate the effectiveness of free radical scavengers. Increased levels of acrylated PEG substantially diminished the number of DPPH radicals present in solution by as much as 80%. Maximum reduction by acrylated PEG was 40% and 30% in ROS and RNS assays, respectively. In all three assays, the presence of non-acrylated PEG had no effect on the concentration of free radicals present, whereas increased amounts of acrylated PEG did reduce the level of radicals present in solution. This confirms that acrylate groups on the PEG chains are responsible for the reactivity with radicals. Although reactive with DPPH and ROS, in neither case did PEGDA reduce the radical concentration as well as ascorbic acid, a well-known, powerful antioxidant. Ascorbic acid

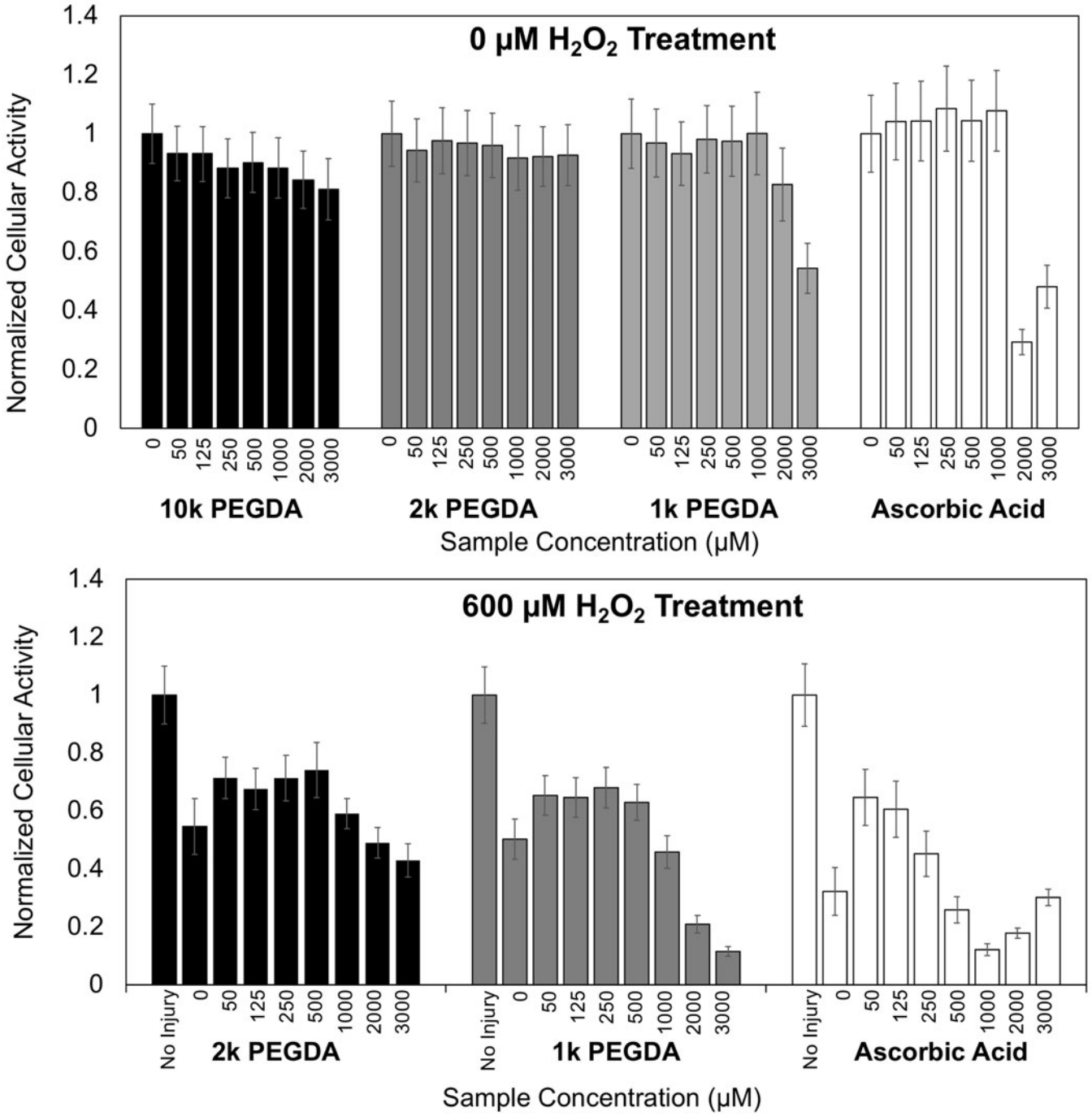


**Figure 5.** Cytotoxicity and Protection of Rat Dermal Fibroblasts. Cellular metabolic activity of rat dermal fibroblasts was assessed in the presence of increasing concentrations of acrylated PEGs and ascorbic acid (top). Cellular metabolic activity of fibroblasts was also measured in the presence of hydrogen peroxide and acrylated PEGs to determine the ability of acrylated PEGs to protect cells from oxidative stress (bottom).

controls were not performed with the RNS assay due to strong interference with the Griess Reaction. Thus, while the PEGDA may serve as a free radical scavenger, it would not be a primary anti-oxidant.

Though acrylate reactivity with various free radicals was investigated, it was necessary to also confirm that covalent crosslinking of acrylate groups is the result of that reactivity. NMR showed that the signal from acrylate groups was substantially reduced after reaction with ROS, indicating these acrylate groups have been consumed, presumably through crosslinking. In contrast, no change in the NMR spectra was observed following exposure to RNS, suggesting that RNS are not sufficient to induce crosslinking of acrylate groups. Further analysis was done with GPC to monitor the change in polymer size distribution that arises from reaction of acrylated PEGs with ROS. An increase in the molecular weight of acrylated PEGs was observed after reaction with ROS as determined by the emergence of higher molecular weight peaks in the elution spectrum after reaction with ROS. Additionally, there was a concomitant decrease in the intensity of the initial reactant peak, which indicates that the initial, low molecular weight polymer species were being converted into crosslinked, higher molecular weight species. Per cent conversion, as calculated from the change in this peak intensity, was dependent on the number of acrylates present and the molecular weight of the starting polymer. The highest conversion was observed for 2k PEGDA (~60%), even when low levels of HRP (and, therefore, radicals) were present. Larger starting polymers (6k and 10k PEGDA) and

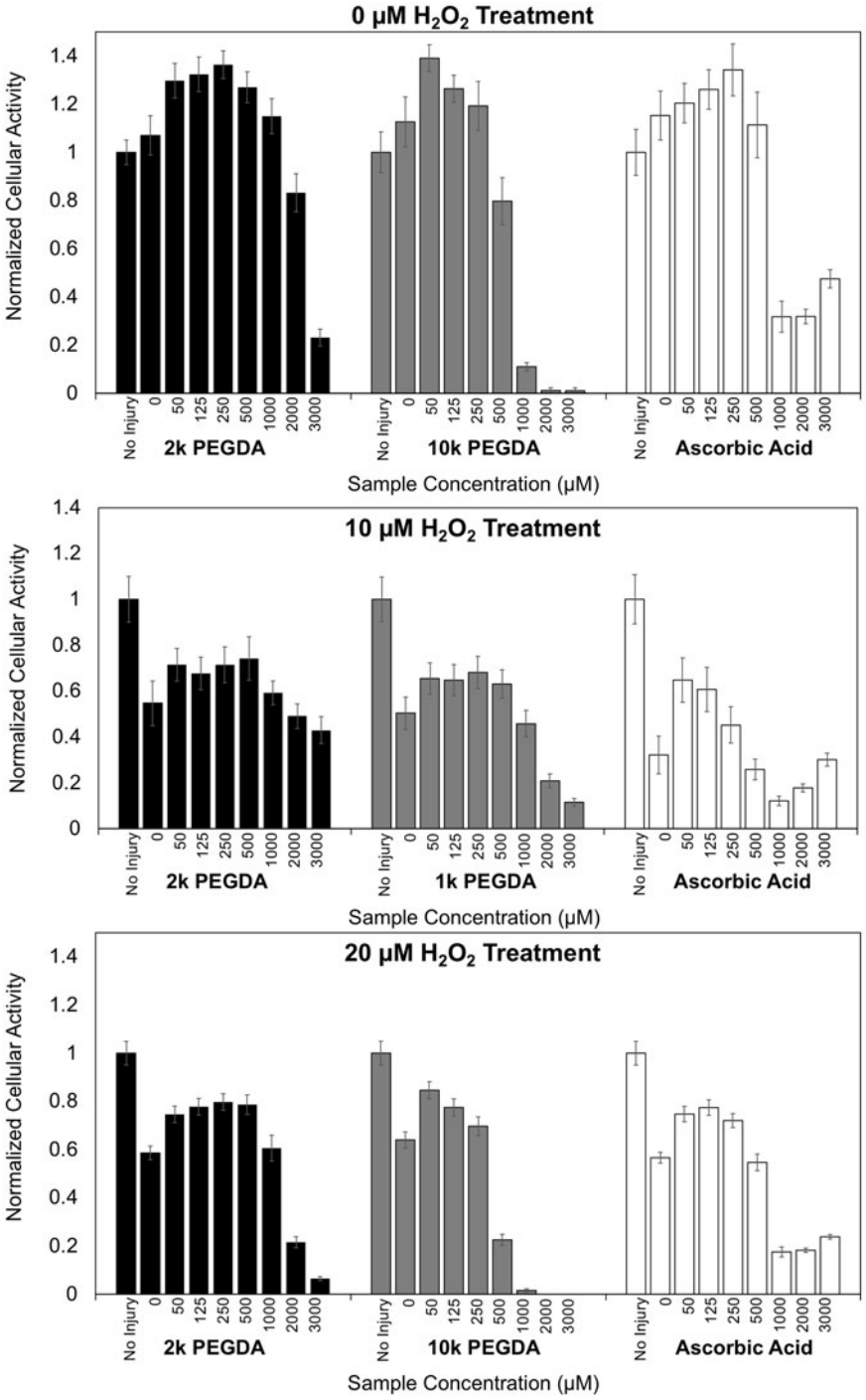


**Figure 6.** Cytotoxicity and Protection of Rat Cortical Neurons. Cellular metabolic activity of rat cortical neurons was assessed in the presence of increasing concentrations of acrylated PEGs and ascorbic acid (top). Cellular metabolic activity of fibroblasts was also measured in the presence of 10 μM (middle) or 20 μM (bottom) hydrogen peroxide and acrylated PEGs to determine the ability of acrylated PEGs to protect cells from oxidative stress.

monoacrylated polymer (2k PEG1A) showed lower conversion, with all sets topping out at approximately 30% conversion. These results suggest that smaller more mobile PEGs with more acrylate groups are able to react with free radicals more quickly, resulting in more crosslinking events than larger acrylated PEGs. Together, these results demonstrate that native ROS are capable of crosslinking acrylated PEGs. Conversely, consistent with the NMR results, no higher molecular weight peaks appeared in the GPC following reaction with RNS (not shown). Thus, within the range of concentrations studied, ROS, but not RNS, are capable of initiating crosslinking of acrylate groups.

To emulate the tissue environment and preliminarily evaluate the potential for free radicals to crosslink the acrylated PEG sufficiently to immobilize it within a tissue, a fibrillar collagen hydrogel model was used as a tissue mimic. Free radicals were introduced to the gels to initiate crosslinking, and an acrylated-PEG fluorophore was included as the payload to allow us to monitor the amount of polymer that remained within the hydrogels. Two free radical systems were used: the photoinitiator Irgacure 2959, to serve as a proof-of-concept for our system, and the HRP-hydrogen peroxide system described earlier. Irgacure 2959 was developed as an efficient photoinitiator for a variety of materials science

applications, whereas the ROS system was selected to expose the polymer to free radicals that may be commonly encountered *in vivo*. The number of radicals produced from Irgacure far exceeds those produced in the ROS conditions, and therefore more acrylate-acrylate crosslinking was expected. An unintended consequence of the elevated production of radicals was their damaging effect on the fluorescence of the acrylate PEG rhodamine. Following exposure with UV, the fluorescence in non-acrylated PEG and PBS conditions was substantially decreased (Figure 4). However, in conditions where acrylate groups were present, very little decrease in fluorescence was observed, indicating that the acrylate groups were able to protect rhodamine molecule by intercepting radicals before they could damage the fluorophore. This speaks to the ability of acrylated PEGs to protect through free radical scavenging. Some fluorophore damage was observed in the ROS system, though to a much lesser degree than in the Irgacure experiments. Because of these differential effects of radicals, raw fluorescence was reported in Figure 4 after radical exposure but prior to washing (wash 0) and after extensive rinsing (wash 5).

After reaction with radicals and washing, hydrogel conditions containing acrylated PEGs retained higher levels of fluorescence than PBS or non-acrylated PEG conditions. This suggests that acrylated PEG has become crosslinked within the hydrogel, making it more difficult for the polymer chains to diffuse out of the gel. Sufficient crosslinking will lead the polymers to form an interpenetrating network trapped within the collagen fibrils. Fluorescence intensity was lower in conditions with non-acrylated PEG or PBS only, demonstrating that increasing the size of the polymer is necessary for immobilization. Further, there was a molecular weight dependence for the residual fluorescence: higher molecular weight acrylated PEGs demonstrated a higher residual fluorescence. In both ROS and Irgacure conditions, much of the 10k PEGDA was immobilized within the hydrogel, while less of the 6k PEGDA and little-to-none of the 2k PEGDA was immobilized. For 2k PEGDA, each crosslinking event increases the molecular weight by 2,000 daltons. For 10k PEGDA, each crosslinking event increases the molecular weight by 10,000 daltons. Thus, 10k PEGDA conditions will reach an 'immobilization threshold' after fewer crosslinking events than the 2k PEGDA. In the ROS conditions, where there are fewer radicals than Irgacure, there was insufficient crosslinking to immobilize 2k PEGDA within the hydrogels. However, in GPC experiments, it was shown that the smaller molecular weight PEGDA had the highest conversion, presumably because the smaller chains are more mobile in solution and can interact with a greater number of radicals before the radicals are extinguished. Moving forward, these results suggest a combination of sizes will be most optimal to achieve immobilization of a polymer network within a tissue: small, fast-reacting acrylated chains that will undergo several crosslinking events, and larger chains that will amplify the size increase upon crosslinking.

ROS and RNS generating systems were selected to introduce free radicals on the benchtop that would commonly be encountered *in vivo*. SNAP presented an especially straightforward method of introducing NO into solutions, as it involves one component, and the donation of NO is achieved by a simple adjustment of temperature and pH. Generation of ROS was less straightforward but achieved through well-understood methods commonly used in ELISA assays and enzymatic polymerisation [25–26]. Acrylated PEGs were readily able to react with the ROS generated with HRP and $H_2O_2$, as seen by the reduction of colour development from the TMB substrate, essentially indicating a competition between the acrylated PEG and the TMB. However, for crosslinking to occur, the radicalised acrylated PEG must then engage with another acrylated PEG, and radicals may expire before this second reaction could occur. Our benchtop system delivers a single bolus of ROS. Free radicals are created all at once, and then there is only a short window while those radicals are active that crosslinking can occur. In contrast, *in vivo* during injury and disease, production of ROS occurs continuously, and there will be a constant source of free radicals and continuous opportunities for crosslinking to occur. During this extended window, a greater number of radicalised acrylated PEGs will be available to interact and thus a greater number of crosslinking events may occur. To adapt our bolus system, in NMR, GPC, and immobilization experiments, an additional component, acetylacetone, was included to prolong the life of those radicals, ensuring that the ROS remain reactive long enough to initiate crosslinking. Collectively, while these systems do not exactly mimic what occurs *in vivo*, these results still represent a strong first step in demonstrating that acrylated PEGs can be successfully immobilized by ROS derived free radicals.

While the primary design goal of our biomaterial approach is targeting, a potential secondary benefit may be protection of cells against oxidative damage by sequestering or otherwise occupying free radicals, as suggested protection of the rhodamine fluorescence. To evaluate cell protection, we first characterised the cytotoxicity of the acrylated PEGs alone to fibroblasts and to neurons in traditional 2-dimensional culture conditions. In preliminary cytotoxicity studies, RDFs tolerated the presence of acrylated PEGs below concentrations of 1000 μM. At concentrations greater than 1000 μM, the toxicity in acrylated PEG conditions mirrored that of ascorbic acid. Similarly, rat cortical neurons tolerated acrylated PEGs up to ~500 μM. Above 500 μM, decreases in cellular activity were observed, coincident with decreases observed in ascorbic acid conditions. In subsequent experiments, without acrylated PEG, exposure to $H_2O_2$ substantially reduced cellular metabolic activity of RDFs and cortical neurons. When even small concentrations of acrylated PEG was present, that injury was reduced. The positive influence of acrylated PEG was dose-dependent up to ~500 μM for RDFs and ~250 μM for cortical neurons. Although oxidative stress may induce cell death by apoptosis as well as through necrosis, autophagy, and other mechanisms, given the molecular weight range of our biomaterial, we are confident that it confers cell protection via action as an exogenous anti-oxidant and not through specific intracellular mechanisms [27–28]. Ultimately, this ability of acrylated PEGs to confer additional protection may present the opportunity to ameliorate injured or diseased tissues through multiple independent mechanisms. Decreasing viability at higher concentrations in protection studies occurred at slightly lower concentrations than in the cytotoxicity studies. We suspect that the additional oxidative stress induced by the $H_2O_2$ may have made the cells more susceptible to toxicity from the acrylated PEGs. Cell death with and without oxidative stress appeared more significant with the 10k PEGDA than the 2k PEGDA and therefore does not appear to be linked to differences or changes in permeability to the PEGDA.

## Conclusion

Herein, we have presented preliminary support of our hypothesis that acrylated PEGs can crosslink upon reaction with free radicals relevant to in vivo pathologies and can deliver and sustain payloads in the presence of those free radicals. Acrylated PEGs have been shown to interact with ROS and RNS, but it appears that only ROS are capable of successfully initiating crosslinking of acrylate groups to one another. Most importantly, acrylated PEGs were successfully immobilized within collagen hydrogels, demonstrating that there is

great potential for acrylated PEGs to serve as a building block for a drug delivery platform which both targets and sustains the presentation of therapeutics to a broad range of injured and diseased tissues. Ongoing and future work aims to identify optimal sizes and configurations of the acrylated carrier polymers and to test these polymers in more advanced tissue mimic models. In addition, we are actively evaluating the efficiency of other free radical sensitive functional groups that may meet or exceed the reactivity of acrylates with ROS and potentially RNS. Ultimately, this proposed system represents a versatile drug delivery platform that targets regions of injured or diseased tissue that could be amended to carry nearly endless therapeutic payloads.

## Disclosure statement

No potential conflict of interest was reported by the authors.

## Funding

The authors would like to thank the New Jersey Commission on Brain Injury Research for their generous support of this research through a pilot research grant (CBIR16PIL015) and a graduate fellowship (CBIR14FEL004). The NIH Biotechnology Training Program (NIH T32 GM008339) and Graduate Assistance in Areas of National Need (GAANN) Fellowship provided additional support for the work presented. A. J. G. was supported by a Busch Biomedical Seed Grant and an American Cancer Society— Institutional Research Grant Early Investigator Pilot Award. Additional support for this work was provided by the National Science Foundation REU in Cellular Bioengineering: From Biomaterials to Stem Cells (NSF EEC 1262924), and the Aresty Undergraduate Research Fellowship Program at Rutgers.

## ORCID

Emily T. DiMartini http://orcid.org/0000-0003-0239-4819
Keana R. Mirmajlesi http://orcid.org/0000-0002-2503-1108
Adam J. Gormley http://orcid.org/0000-0002-2884-725X
David I. Shreiber http://orcid.org/0000-0001-8248-419X

## References

[1] Bae YH, Park K. Targeted drug delivery to tumors: myths, reality and possibility. J Control Rel. 2011;153:198–205.
[2] Cheng Z, Al Zaki A, Hui JZ, et al. Multifunctional nanoparticles: cost versus benefit of adding targeting and imaging capabilities. Science. 2012;338:903–910.
[3] Banerjee A, Pathak S, Subramanium VD, et al. Strategies for targeted drug delivery in treatment of colon cancer: current trends and future perspectives. Drug Dis Today. 2017;22:1224–1232.
[4] Kakde D, Jain D, Shrivastava V, et al. Cancer therapeutics - opportunities, challenges, and advances in drug delivery. J Appl Pharm Sci. 2011;1:01–10.
[5] Toporkiewicz M, Meissner J, Matusewicz L, et al. Toward a magic or imaginary bullet? Ligands for drug targeting to cancer cells: principles, hopes, and challenges. Int J Nanomed. 2015;10:1399–1414.
[6] Kwon IK, Lee SC, Han B, et al. Analysis on the current status of targeted drug delivery to tumors. J Control Rel. 2012;164:108–114.
[7] Vasir JK, Labhasetwar V. Targeted drug delivery in cancer therapy. Technol Cancer Res Treat. 2005;4:363–374.
[8] O'Connell KM, Littleton-Kearney MT. The role of free radicals in traumatic brain injury. Biol Res Nursing. 2013;15:253–263.
[9] Poprac P, Jomova K, Simunkova M, et al. Targeting free radicals in oxidative stress-related human diseases. Trends Pharmacol Sci. 2017;38:592–607.
[10] Kehrer JP, Klotz LO. Free radicals and related reactive species as mediators of tissue injury and disease: implications for Health. Crit Rev Toxicol. 2015;45:765–798.
[11] Zhang PY, Xu X, Li XC. Cardiovascular diseases: oxidative damage and antioxidant protection. Eur Rev Med Pharmacol Sci 2014;18:3091–3096.
[12] Valko M, Leibfritz D, Moncol J, et al. Free radicals and antioxidants in normal physiological functions and human disease. Int J Biochem Cell Biol. 2007;39:44–84.
[13] Bryan N, Ahswin H, Smart N, et al. Reactive oxygen species (ROS) – a family of fate deciding molecules pivotal in constructive inflammation and wound healing. Ecm. 2012;24:249–265.
[14] Shi S, Xue F. Current antioxidant treatments in organ transplantation. Oxidat Med Cell Longevity. 2016;2016:1.
[15] Knight JA. Free Radicals, Antioxidants, and the Immune System. Annal Clin Lab Sci. 2000;30:145–158.
[16] Pham-Huy LA, He H, Pham-Huy C. Free Radicals, Antioxidants in Disease and Health. Int J Biomed Sci. 2008;4:89–96.
[17] Cowie JMG, Arrighi V. Polymers: Chemistry and Physics of Modern Materials. 3 ed. CRC Press. 2007.
[18] Lin CC, Anseth KS. PEG hydrogels for the controlled release of biomolecules in regenerative medicine. Pharm Res. 2009;26:631–643.
[19] Florence TM. The role of free radicals in disease. Aust N Z J Ophthalmol. 1995;23:3–7.
[20] Lobo V, Patil A, Phatak A, C, et al. antioxidants and functional foods: Impact on human health. Pharm Rev. 2010;4:110–126.
[21] Xu SY, Wu YM, Ji Z, et al. A modified technique for culturing primary fetal rat cortical neurons. J Biomed Biotechnol. 2012;2012:803930.
[22] Sharma OP, Bhat TK. DPPH antioxidant assay revisited. Food Chemistry. 2009;113:1202–1205.
[23] Titheradge MA. The enzymatic measurement of nitrate and nitrite. Methods Mol Biol. 1998;100:83–91.
[24] Mironi-Harpaz I, Wang DY, Venkatraman S, et al. Photopolymerization of cell-encapsulating hydrogels: crosslinking efficiency versus cytotoxicity. Acta Biomaterialia. 2012;8:1838–1848.
[25] Gormley AJ, Chapman R, Stevens MM. Polymerization amplified detection for nanoparticle-based biosensing. Nano Lett. 2014;14:6368–6373.
[26] Kobayashi S, Uyama H, Kimura S. Enzymatic polymerization. Chem Rev. 2001;101:3793–3818.
[27] Ryter SW, Kim HP, Hoetzel A, et al. Mechanisms of cell death in oxidative stress. Antioxid Redox Signal. 2007;9:49–89.
[28] Filomeni G, Zio DD, Cecconi F. Oxidative stress and autophagy: the clash between damage and metabolic needs. Cell Death Differ. 2015;22:377–388.